



Mechanical properties of thermally treated granite subjected to different multi-stage unloading paths

Peng Kang¹ · Zhang Jing² · Liu Hao² · Gao Xicai³ · Zheng Chunshan⁴

Received: 1 August 2021 / Accepted: 22 October 2022 / Published online: 9 January 2023
© The Author(s), under exclusive licence to Springer-Verlag GmbH Germany, part of Springer Nature 2023

Abstract

The aim of this study is to investigate deformation characteristics of thermally subjected granite at different rates of unloading confining pressure. For this purpose, by using a RTX-3000 high-temperature and high-pressure triaxial rock testing machine, a conventional triaxial compression test and a triaxial unloading confining pressure test under constant deviatoric stress were conducted on granite after being heated to 800 °C and cooled naturally. The results show that, compared with the conventional triaxial compression test, the stress–strain curve in the unloading confining pressure test showed an obvious yield platform, in which points of obvious stress drop were observed and rock had obvious characteristics of brittle failure. In the initial stage of unloading confining pressure, volumetric strain increased slightly, and then it rose rapidly till the rock samples were damaged as confining pressure was reduced to a certain extent. In this process, the dilatancy angle of the rock samples rapidly increased with the decrease of confining pressure, followed by a sharp drop immediately after reaching a certain value. Strain-pressure compliance of the rock samples changed slightly in the first three stages in each group of the tests and rapidly rose from the fourth stage. Different from the conventional triaxial compression test, tangent modulus of the rock samples rapidly decreased at the beginning of unloading and then attenuated with leaps. Elastic modulus and Poisson's ratio of the rock samples changed slightly at the beginning of unloading and rapidly reduced with the further decrease of confining pressure till the rock samples were damaged. This study results elucidate the mechanical properties of rocks affected by high temperatures and provide theoretical support to clarify the stability of rocks in deep rock formations after heat exposure.

Keywords Granite · High temperature · Unloading in different stages · Strain-pressure compliance · Mechanical properties

Introduction

Rock, as a natural material with various defects (such as primary micro-fractures), is commonly used in different engineering applications, especially for water conservancy and hydropower, civil engineering and underground mining

that involves rock and coal (Zou et al. 2021, 2022a, b; Kim et al. 2021; Dou et al. 2021; Dong et al. 2021). Widespread acceptance in rocks, there are primary defects, such as joints, microcracks and pores. At high temperature, due to anisotropy and inhomogeneity of thermal expansion of various mineral compositions in all geomaterials, the internal structure of geomaterials will change, such as the increase, propagation and coalescence of microcracks. In rocks, elastic modulus and mechanical strength decrease (Witherspoon, 2011; Witherspoon et al. 2006; Tsang et al. 2005; Aversa et al. 1998; Chaki et al. 2008; Liu et al. 2014; Yu et al. 2015; Popov et al. 2016; Kayabasi et al. 2003), while permeability increases (Cevik et al. 2011; Dobson et al. 2002; Vázquez et al. 2015; Yu et al. 2016; Hashemi et al. 2015), thermal expansion degrades mechanical properties of rock to some extent. These changes of rock may lead to instability and failure (Hashemi et al. 2015; Brotons et al. 2013; Liu et al. 2021a, b). Numerous scientists have carried out relevant

✉ Liu Hao
liuhaocqu@cqu.edu.cn

¹ School of Resources and Safety Engineering, Central South University, Changsha 410083, China

² College of Aerospace Engineering, Chongqing University, Chongqing 400044, China

³ State Key Laboratory of Coal Resources in Western China, Xi'an University of Science and Technology, Xi'an 710000, China

⁴ School of Safety Science and Engineering, Anhui University of Science and Technology, Huainan 232001, China

experimental researches on changes of mechanical properties of rock after high-temperature treatment. By performing a mechanical test under uniaxial compression on the thermally subjected granite at 20–600 °C, Xu (2000) concluded that 75 °C is the threshold temperature for compressive strength of granite, while 200 °C is the threshold temperature for elastic modulus under uniaxial compression. Houpert (1979) and Wong (1982) considered that different rock shows different peak strengths under each temperature, and peak strength of most of rock reduces at higher temperature. Lau (1995) studied the change laws of some mechanical and deformation parameters of granite with temperature under low confining pressure. Many scholars have studied physical and mechanical properties of rock after being subjected to high-temperature treatment; however, existing research mainly focuses on loading paths in uniaxial compression, while the conventional triaxial loading is rarely researched, let alone in unloading path.

In fact, rock mass mainly undergoes unloading stress paths during underground excavation and failure of support structures, and its mechanical behaviors are greatly different from those under conventional loading (Wu et al. 2004; Xie et al. 2004; Ranjan et al. 2021; Liu et al. 2021a, b; Zou et al. 2022c, a, b). Lau (2004) put forward that mechanical parameters under loading paths cannot be used to describe unloading behaviors and it is proper to use the unloading mechanical parameters. Chai (2011) conducted an experimental research on effects of different unloading rates on deformation parameters and failure modes of rock and found that, with rising the unloading rate, the elastic modulus of the rock and the damage of the rock decrease, and the unloading amount of confining pressure increases. Under rock failure, the larger the magnitude of unloading of confining pressure, the more sharply the rock is damaged and the more intensely the energy is released. Yang (2017) conducted an unloading test of rock under different initial confining pressures by using an MTS815 servo-controlled testing machine, and analyzed the characteristics of deformation and energy changes. Based on this, they obtained that the increase rates of energy and stress of the rock samples before peak rise with the initial confining pressure, while those after peak are hardly affected by the initial confining pressure.

Above studies on mechanical properties under unloading do not take the influences of high-temperature damages to rock. Recently, Meng (2018) realized the importance of this problem, and carried out conventional triaxial UCP tests on sandstone at different temperatures from 20 to 150 °C, and obtained valuable research results. Previous studies have deepened the understanding of high-temperature mechanical properties and unloading law of rock, but in most of the previous studies, only the relationships of high temperature and unloading with mechanical properties of rock are independently researched, and both aspects are rarely considered

at the same time. Therefore, the purpose of this research is to study the mechanical properties and changes of deformation parameters of the granite samples thermally subjected at 800 °C and naturally cooled at different unloading rates. To this end, the granite samples were tested in five stages with different unloading rates (different unloading rates in different stages) after being heated, so as to analyze change characteristics of mechanical properties and change laws of deformation parameters. The study results elucidate the mechanical properties of rocks that are affected by high temperatures, providing theoretical support to clarify the stability of rocks that are affected by high temperatures in deep ground.

Rock sample preparation and test procedures

Rock sample preparation

Granite in this research was taken from Xincheng Village, Laizhou City, Shandong Province, China. Owing to the diameter of a drilled core was 65 mm, the rock core obtained from a borehole could not be reprocessed. For this reason, the rock samples were obtained from a large intact rock without obvious cracks or fractures at the elevation of – 1,080 m. The rock samples were 100 mm high and 50 mm in diameter, and categorized as fine-grained single-crystal granite bearing biotite, as shown in Fig. 1a. Field observation showed that granite had good integrity and dense texture. SEM test results demonstrated that the samples were uniform and almost free of microcracks, as shown in Fig. 2a and b. According to the standard requirements (Franklin et al. 1979) of the International Society for Rock Mechanics, the samples were tested to control their parallelism within ± 0.05 mm and surface flatness within ± 0.02 mm. A SRX2-4-10 high-temperature box type resistance furnace (Fig. 3) was used for heating the samples using wire coils, with rated power, voltage and temperature of 2.5 kW, 220 V and 1000 °C. The rock samples were kept for 6 h at constant temperature after raising the temperature to 800 °C at the rate of 10 °C/min to uniformly heat the rock samples and then they were taken out after being naturally cooled to room temperature in the furnace. The rock samples changed from offwhite to white after high-temperature treatment, as shown in Fig. 1b and sizes and physical properties of four groups of rock samples are listed in Table 1.

To study changes of microstructures of the rock samples due to high-temperature treatment, scanning electron microscope (SEM) analysis was performed on the rock samples at room temperature and thermally subjected at 800 °C. The EM-30AX Plus SEM with resolution of 5 nm was used. A small number of microcracks

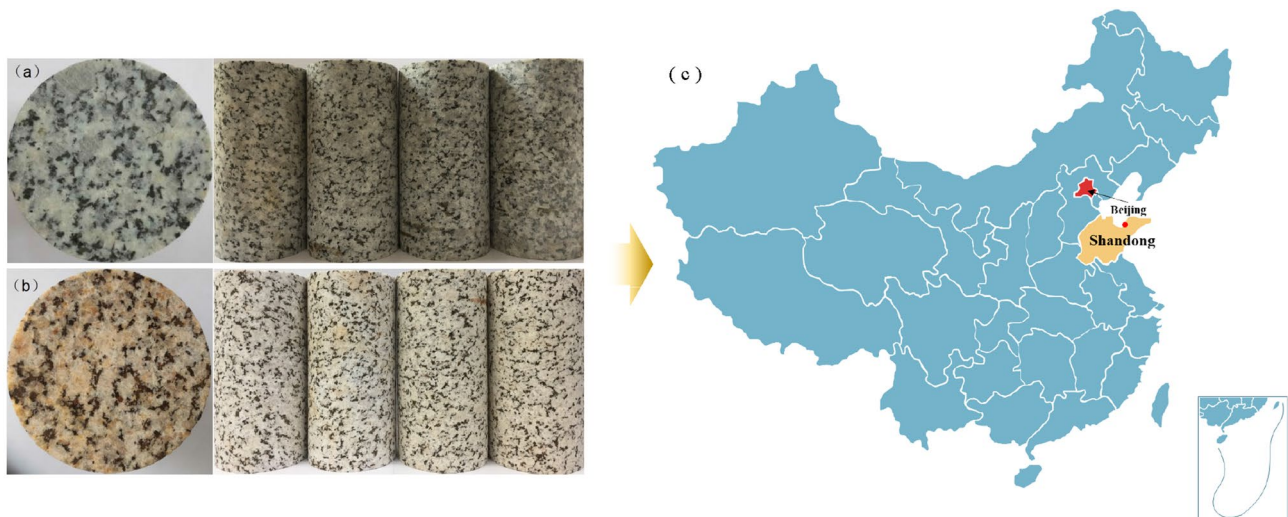
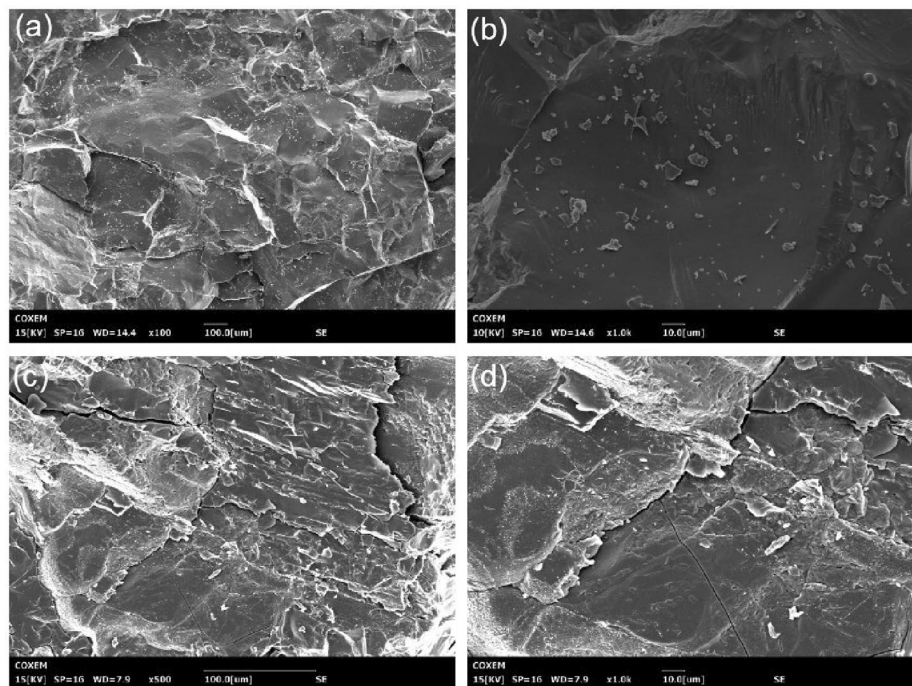


Fig. 1 Comparisons of the granite samples before and after high-temperature treatment: **a** the rock samples at room temperature; **b** the rock samples after high-temperature treatment at 800 °C; **c** Xincheng Village, Laizhou City, Shandong Province

Fig. 2 SEM test of the rock samples. **a, b** The granite samples at room temperature; **c** and **d** The granite samples thermally subjected at 800 °C



(Fig. 2a, b) were observed on the rock samples without being thermally subjected, which meant that the granite samples showed almost intact microstructures in their initial states. Crack propagation divided many crystals into small pieces (Fig. 2c, d), while gradual failure of microstructures finally changed macroscopic physical and mechanical properties of rock.

Test equipment

An RTX-3000 high-temperature and high-pressure triaxial rock testing machine produced by the GCTS Company in the United States was used in the tests. Maximum allowable axial load by the system was 3000 Kn (Fig. 4a). In the test process, circumferential deformation of the rock samples

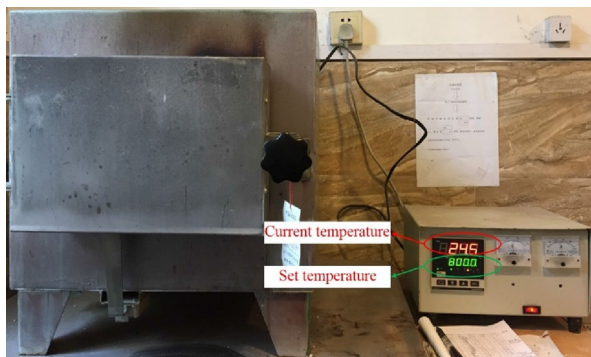


Fig. 3 The SRX2-4-10 high temperature box type resistance furnace

Table 1 Basic parameters of the granite samples

| Rock sample | Diameter/mm | Height/mm | Mass/g | Density/ (g·cm ⁻³) |
|-------------|-------------|-----------|--------|-----------------------------------|
| A | 50.18 | 100.00 | 523.82 | 2.65 |
| B | 49.16 | 99.56 | 503.30 | 2.66 |
| C | 49.88 | 99.64 | 521.48 | 2.68 |
| D | 49.98 | 99.68 | 519.64 | 2.66 |

was measured by a ring extensometer linked with chains installed in the middle of the samples, while the axial deformation was measured by using two axial extensometers, as displayed in Fig. 4b. In this test, loading and unloading tests were conducted by controlling deviatoric stress. In other words, deviatoric stress ($\sigma_1 - \sigma_3$) was kept constant in the test. Displacement control mode for loading was used in the triaxial loading stage and axial pressure was loaded at the rate of 0.02 mm/min, while stress control mode was adopted in the unloading stage. The test process was controlled by a computer and test data were automatically collected.

Test procedures

Different stress paths can be selected to unload confining pressure. According to the changes of deviatoric stress during UCP, stress paths for UCP of rock can be classified into the following categories, as shown in Fig. 5. In the figure, OA represented the stress path in the conventional TC test, that is, under constant confining pressure, axial pressure was continuously loaded till the samples were damaged (the dotted line in the figure was the hypothetical nonlinear strength criterion). OB indicated the stress path when axial pressure was increased while UCP till the samples were damaged; OC suggested the stress path that confining pressure was unloaded under constant axial pressure till the samples were damaged. Moreover, OD represented the stress path under which confining pressure was unloaded till the samples were damaged under constant deviatoric stress. To unload confining pressure under unchanged deviatoric stress was in essence to unload axial and confining pressures equivalently. In existing researches, most of scholars have studied paths OB and OC, while there were few researches under constant deviatoric stress (path OD). Deng (2017) studied the relationship between unloading characteristics of sandstone and pore water pressure under constant deviatoric stress. Different test laws could be obtained under different loading paths and unloading stress paths, which was one of the important reasons for obtaining non-uniform laws in existing unloading tests. Under the above three stress paths, the main difference was the changes of axial pressure during UCP, while the UCP test under constant deviatoric stress was rarely studied at present. Therefore, the effects of rate of UCP on mechanical properties of granite under unloading were investigated by selecting the stress path that confining pressure was unloaded under unchanged deviatoric stress (OD in Fig. 5).

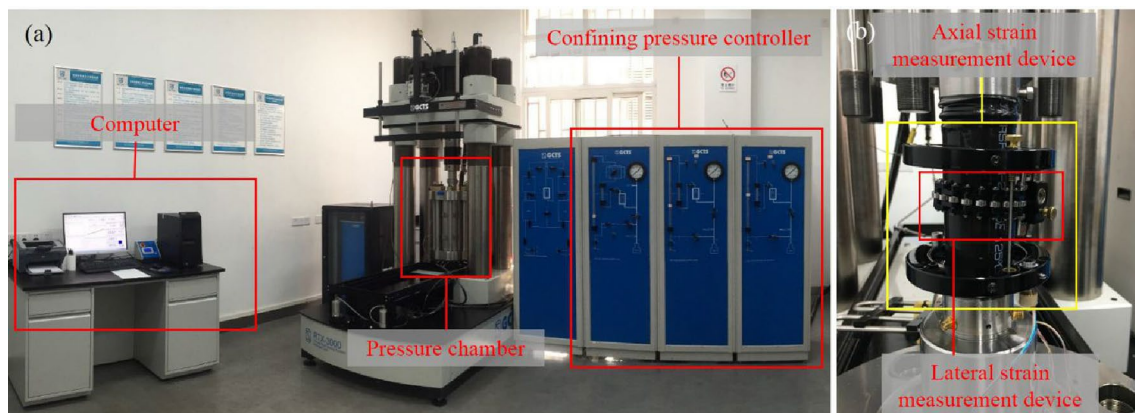


Fig. 4 Test equipment (Peng et al. 2019). **a** The RTX-3000 high-temperature and high-pressure triaxial rock testing system; **b** Strain gauge

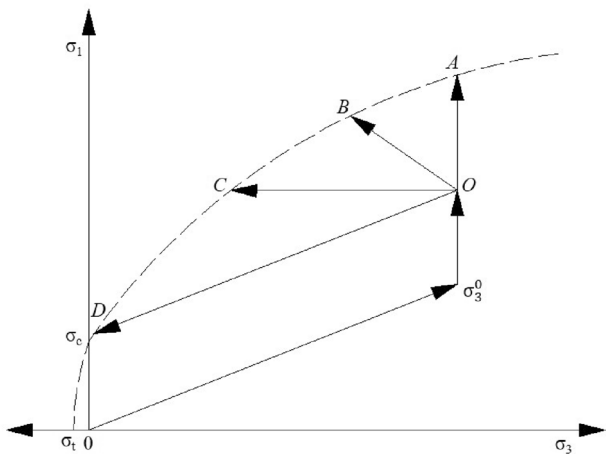


Fig. 5 Sketch map of different stress paths for UCP

The test scheme was discussed as follows: firstly, the conventional triaxial test under confining pressure of 10 MPa was conducted to determine the peak strength of the samples after being heated at 800 °C and naturally cooled. Then, the test at different unloading rates in different stages was carried out for determining mechanical properties of rock and the design schemes are displayed in Table 2. The steps for the UCP test of the rock samples at different unloading rates in different stages were presented as follows:

1. By using stress control mode, confining pressure and axial pressure were loaded to the preset value of 10 MPa and increase rates thereof were both kept at 2 MPa/min during loading.
2. After applying confining pressure to the preset value, the displacement control mode was used to continuously apply axial load at the loading rate of 0.02 mm/min to 60% of ultimate bearing capacity of the rock samples under such a confining pressure. Then, stress of the samples was stabilized for 5 min.
3. Under constant deviatoric stress, confining pressure was removed by unloading in different stages.

4. The unloading of confining pressure was stopped immediately after stress in the rock samples sharply dropped. Under the condition, the rock samples were completely damaged and the test was over.

Test results

Characteristics of stress–strain curves of the rock samples under the conventional TC

Figure 6 shows the deviatoric stress–strain curves of the thermally subjected granite samples under the conventional triaxial loading when confining pressure is 10 MPa. Figure 7 illustrates comparisons of stress–strain curves during the conventional triaxial loading test and UCP test under constant deviatoric stress on the rock samples when initial confining pressure is same (10 MPa). In the figures, the mode for loading confining pressure on the rock samples is shown as follows: after increasing confining pressure to the preset value of 10 MPa through mechanical pressurization, confining pressure keeps unchanged and axial pressure is loaded by using stress control mode at the rate of 2 MPa/min. It can be seen from Fig. 6 that when confining pressure is constant,

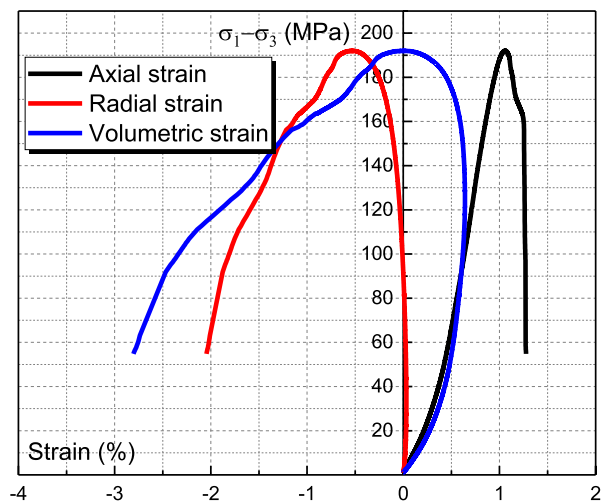


Fig. 6 Stress–strain curves of the granite under the conventional triaxial loading

Table 2 Test schemes for unloading in different stages on the granite samples

| Test group | Axial pressure/MPa | Confining pressure/MPa | Rate of UCP/(kPa·s ⁻¹) | | | | |
|------------|--------------------|------------------------|------------------------------------|---------|---------|---------|---------|
| | | | Stage 1 | Stage 2 | Stage 3 | Stage 4 | Stage 5 |
| A | 125 | 10 | 1.5 | 3.0 | 7.5 | 9.5 | 11.5 |
| B | 125 | 10 | 11.5 | 9.5 | 7.5 | 3.0 | 1.5 |
| C | 125 | 10 | 1.5 | 3.0 | 7.5 | 3.0 | 1.5 |
| D | 125 | 10 | 11.5 | 9.5 | 7.5 | 9.5 | 11.5 |

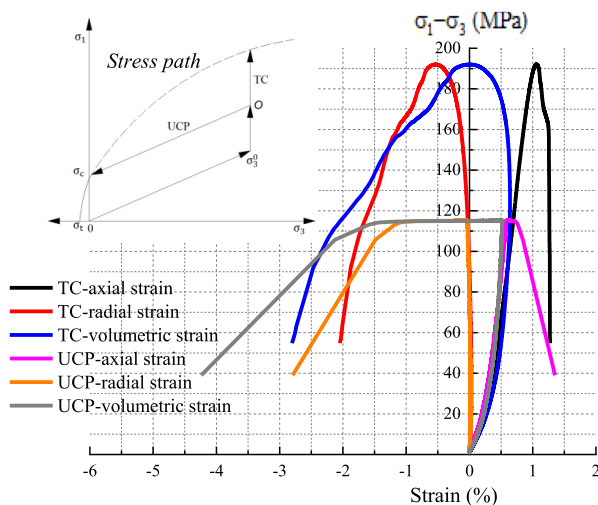


Fig. 7 Stress–strain curves of the granite under two stress paths

stress–strain curve of the thermally subjected granite samples under TC undergoes four stages, i.e., compaction, elastic, yield and failure stages. Short course of compaction stage, and the stress–strain curve is slightly concave. The reason is that under the action of high temperature, part of water in the rock evaporates and the air expands. Moreover, the existence of confining pressure compacts or in rock, thus the rock is compressed. In the obvious elastic stage, before axial strain reaches the peak, the relationship between stress and strain is approximately linear, showing elastic characteristics of the rock samples. Before the stress reaches the peak, stress shows a nonlinear relationship with strain and elastic modulus of the rock samples constantly decreases with the increase of strain, presenting yielding phenomenon. After stress reaches the peak, axial strain is maximized, and fractures in the rock samples coalesce and form macrocracks, so that the rock samples lose bearing capacity and the stress decreases. Therefore, the rock samples demonstrate characteristics of brittle failure. As shown in Fig. 6, in the conventional TC test, volumetric strain begins to recover at 60% of peak stress. Therefore, it is determined that deviatoric stress in the UCP test under constant deviatoric stress should remain unchanged at 60% of peak stress in the conventional TC test of the rock samples.

Figure 7 demonstrates characteristic stress–strain curves of the rock samples in the conventional TC test and UCP test under constant deviatoric stress. It can be observed from the figure that compared with conventional TC test, stress–strain curves in the UCP test under constant deviatoric stress show basically same deformation characteristics before reaching the peak, while deformation in the peak areas is significantly different. In the process of keeping deviatoric stress constant and gradually reducing confining pressure, there is no obvious peak point, while an obvious yield platform appears.

With decreasing the confining pressure, the slope of the curve decreases and the strain increases, so that the curve is appropriately flat. In this process, the volume expands and the deformation increases sharply until it breaks.

Characteristics of stress–strain curves under UCP in different stages at different rates

As illustrated in “Characteristics of stress–strain curves of the rock samples under the conventional TC”, volumetric strain begins to rotate at about 60% of peak strength, and deviatoric stress is 115.2 MPa. In order to facilitate analysis and operation, the deviatoric stress values 115 MPa in the test process. Therefore, the initial axial stress under UCP in this study is about 60% of peak strength in the TC test. Figure 8 demonstrates the curves of the relationship between deviatoric stress and strain of granite after being subjected at high temperature and cooled naturally in the triaxial UCP test in different stages at different unloading rates. It can be seen from Fig. 8 that the stress–strain curves can be divided into the following three stages according to change trend of deviatoric stress–strain curve.

1. Confining pressure loading stage, namely compaction stage. In this stage, strain increases obviously. When confining pressure is loaded from 0 to 10 MPa, circumferential strain constantly rises and the deviatoric stress–strain curve is downwardly concave. This shows that increase rate of strain decreases, that is, the increase rate of circumferential strain is large in the initial stage of loading confining pressure and decreases as confining pressure approaches to 10 MPa. In this stage, axial strain and volumetric strain show a same change trend with circumferential strain, all shown as decreased increase rate of strain, which results from closure of fractures in the rock samples. After high-temperature treatment, the water evaporation of the rock samples and the dehydration of minerals lead to the decrease of water content, the increase of the porosity, and the compaction of the pores and fractures during loading process. In the three test groups, radial strains are slightly different when confining pressure rises to 10 MPa.
2. Axial pressure loading stage, namely elastic stage. When confining pressure is constant at 10 MPa and axial pressure is continuously applied to 60% of peak strength in the TC test, axial strain constantly rises, while radial strain decreases slightly. It can be observed from Fig. 6 that deviatoric stress–strain of the granite in this stage is nearly linear, so elastic modulus can be regarded as a constant and rock deformation shows obvious elastic deformation. In this stage, irrecoverable deformation of rock has not appear yet.

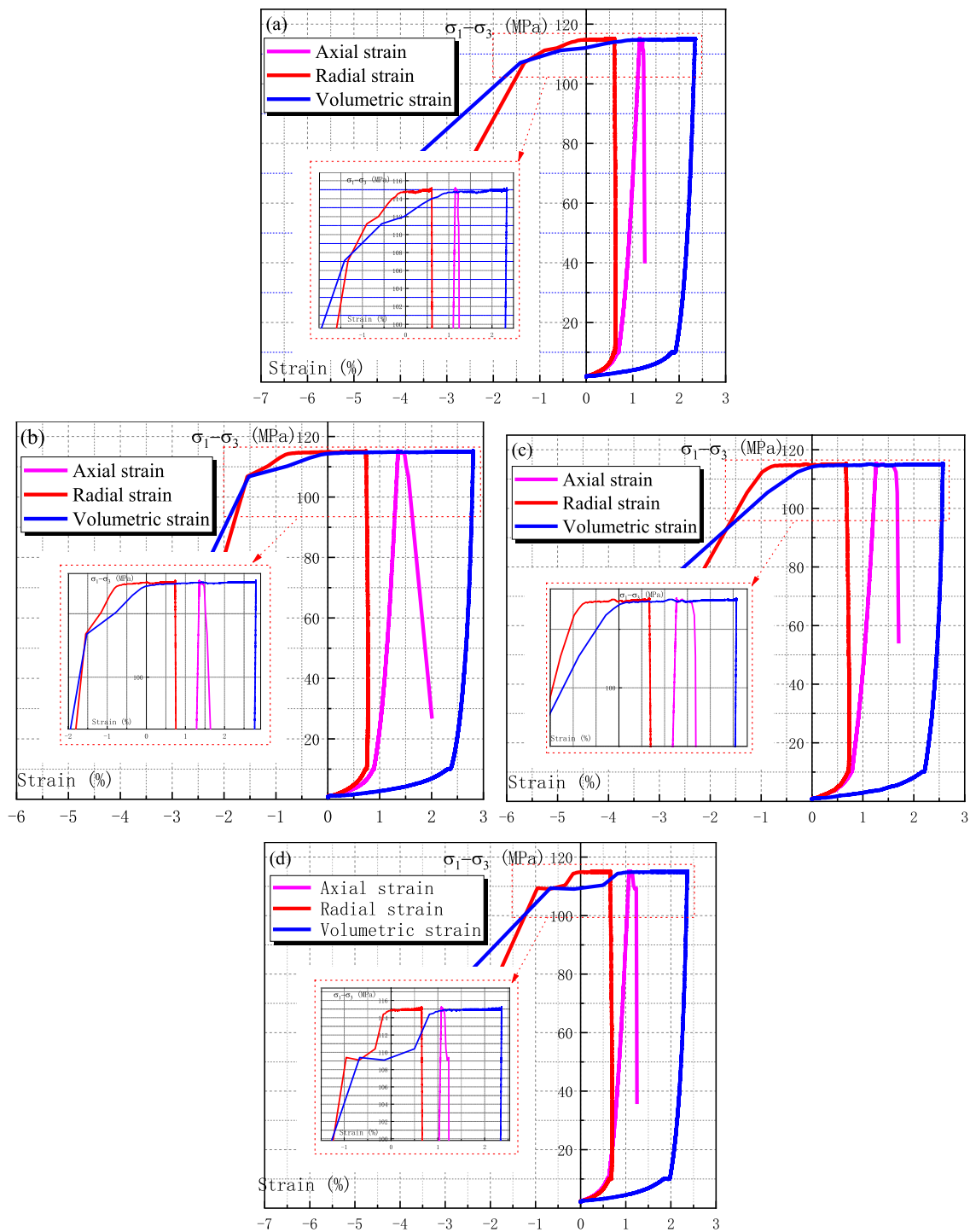


Fig. 8 Stress–strain curves under UCP at different rates in different stages. **a** Test group A; **b** Test group B; **c** Test group C; **d** Test group D

3. Confining pressure unloading stage. Yield stage of rock is obvious in the process of keeping deviatoric stress constant and gradually reducing confining pressure. Deviatoric stress–strain curve is almost flat and axial deformation changes relatively slowly while radial deformation rapidly increases, and the rock sam-

ples show irrecoverable plastic deformation. With the decrease of confining pressure, original cracks in the samples propagate and coalesce or new cracks initiate, and finally coalesced cracks sufficient to damage the whole rock samples are formed. In this process, rock volume expands and deformation of rock increases

sharply after the confining pressure decreases to a certain extent, during which points of obvious stress drop can be observed.

Discussion

Effects of different unloading rates on the relationship between confining pressure and strain

Figure 9 illustrates the curves of the relationship between confining pressure and volumetric strain during UCP on granite. In this research, because confining pressure begins to be unloaded at different moments in each test group, strains of the rock samples change in different groups at the same moment. In order to facilitate the analysis of the change trend between confining pressure and volumetric strain, the relationships between confining pressure and strain in unloading stage of the four test groups are normalized, so that strain at the starting point of unloading is same. Such processing is equivalent to shifting the curve of the relationship between confining pressure and volumetric strain leftwards or rightwards in the figure, which does not change the variation trend of confining pressure with volumetric strain under different unloading modes in different stages. Chai (2011) conducted an experimental research on effects of different unloading rates on deformation parameters and failure modes of rock and found that, with rising the unloading rate, the elastic modulus of the rock and the damage of the rock decrease, and the unloading amount of confining pressure increases. As shown in Fig. 9, in the initial stage of UCP, volumetric strain increases slightly, so the

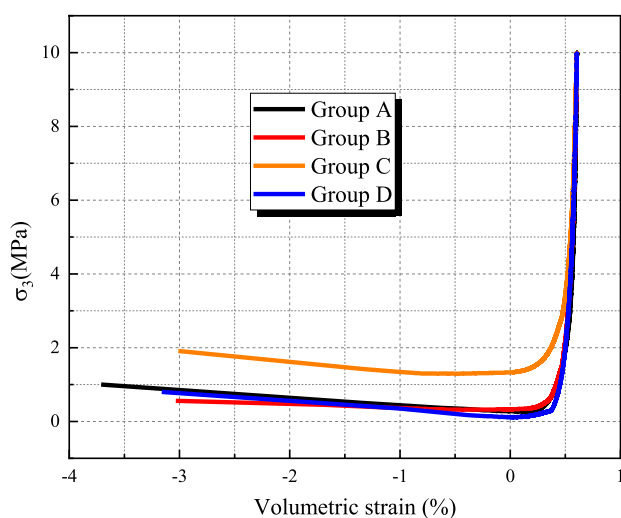


Fig. 9 Curves of the relationship between confining pressure and volumetric strain in unloading stage of the rock samples

rock samples are still in the linearly elastic stage. With the further reduction of confining pressure, volumetric strain and confining pressure do not show the linear relationship any more, suggesting that irrecoverable plastic deformation of the rock samples begins to appear. After confining pressure decreases to a certain degree, volumetric strain rapidly rises. In this process, cracks in the rock samples gradually initiate, propagate, coalesce and finally form cracks running through the whole rock sample, resulting in failure of the rock. It can be qualitatively observed from Fig. 9 that such a deformation law of the rock is similar under different paths. However, it is noted that the curve of the rock samples under stress path in test group C is located at the top, and the confining pressure decreases least. This indicates that in comparison with the other three groups of UCP tests in different stages, the thermally subjected granite samples are most easily to be damaged under the UCP stress path in different stages in group C. As we all know, failure of the rock samples during UCP is caused by rapid expansion of volume, which suggests that the rock samples expand the largest and are most likely to be damaged under the stress path in the group C.

Table 3 lists variations of confining pressure and strain in each stage under different stress paths. It can be obviously seen from the table that the rock samples in the test groups A, B and D are all damaged in the fifth stage, while those in the test group C are damaged in the fourth stage, which again indicates that the rock samples are most easily damaged under stress path in this test group.

Therefore, the decrease rate $\Delta\sigma_3$ of confining pressure at failure in unloading is defined to reflect difficulty of failure and with rising the value, the damage degree of the rock increases.

$$\Delta\sigma = \frac{(\sigma_0 - \sigma_3)}{\sigma_0}, \quad (1)$$

where σ_0 and σ_3 represent the confining pressures in the initial unloading stage and at failure, respectively.

Table 4 illustrates the maximum and minimum principal stresses and decrease rates of confining pressure at failure in unloading in each test group. It can be quantitatively concluded from the maximum and minimum principal stresses at failure of the rock samples in unloading test in Table 4 that the confining pressure of the rock samples decreases least (to 87%) in the group C. This indicates that the thermally subjected rock samples are most likely to be damaged under the UCP path in this stage. In addition, it can be seen that among the volumetric strain increments corresponding to the four test groups, the volumetric strain increment in the test group C is the largest. This means that the granite expands most intensely under the stress path in this test group and the magnitude of unloading required to achieve failure is the

Table 3 Variations of strain and confining pressure in different unloading stages

| Test group | Parameter | Stage 1 | Stage 2 | Stage 3 | Stage 4 | Stage 5 |
|------------|--|---------|---------|---------|----------|----------|
| A | Magnitude of unloading of confining pressure (MPa) | 0.45 | 0.9 | 2.25 | 2.85 | 3.28 |
| | Axial strain increment (10^{-3}) | 0.004 | - 0.003 | - 0.004 | 0.029 | 0.562 |
| | Radial strain increment (10^{-3}) | - 0.013 | - 0.037 | - 0.125 | - 0.318 | - 5.747 |
| | Volumetric strain increment (10^{-3}) | - 0.022 | - 0.076 | - 0.25 | - 0.596 | - 10.768 |
| B | Magnitude of unloading of confining pressure (MPa) | 3.45 | 2.85 | 2.25 | 0.9 | 0.24 |
| | Axial strain increment (10^{-3}) | - 0.023 | 0.004 | 0.058 | 0.114 | 0.583 |
| | Radial strain increment (10^{-3}) | - 0.223 | - 0.397 | - 0.773 | - 1.253 | - 7.781 |
| | Volumetric strain increment (10^{-3}) | - 0.459 | - 0.774 | - 1.456 | - 2.346 | - 14.751 |
| C | Magnitude of unloading of confining pressure (MPa) | 0.9 | 1.8 | 4.5 | 1.5 | - |
| | Axial strain increment (10^{-3}) | 0.032 | 0.005 | - 0.023 | 3.267 | - |
| | Radial strain increment (10^{-3}) | - 0.066 | - 0.169 | - 1.135 | - 12.733 | - |
| | Volumetric strain increment (10^{-3}) | - 0.096 | - 0.328 | - 2.251 | - 21.855 | - |
| D | Magnitude of unloading of confining pressure (MPa) | 2.3 | 1.9 | 1.5 | 1.9 | 2.29 |
| | Axial strain increment (10^{-3}) | - 0.018 | - 0.001 | 0.006 | 0.027 | 0.472 |
| | Radial strain increment (10^{-3}) | - 0.133 | - 0.181 | - 0.193 | - 0.412 | - 5.458 |
| | Volumetric strain increment (10^{-3}) | - 0.278 | - 0.357 | - 0.375 | - 0.783 | - 10.295 |

Table 4 The maximum and minimum principal stresses at failure under unloading conditions

| Test group | Initial confining pressure σ_0 (MPa) | At failure σ_3 (MPa) | At failure σ_1 (MPa) | Volumetric strain increment (10^{-3}) | (σ_3/σ_0) (%) | $\Delta\sigma_3$ (%) |
|------------|---|-----------------------------|-----------------------------|---|---------------------------|----------------------|
| A | 10 | 0.27 | 115.27 | 11.730 | 2.7 | 97.3 |
| B | 10 | 0.31 | 115.31 | 19.786 | 3.1 | 96.9 |
| C | 10 | 1.30 | 116.30 | 24.530 | 13.0 | 87.0 |
| D | 10 | 0.11 | 115.11 | 12.388 | 1.1 | 98.9 |

least. Under other paths, the expansion is relatively stable and confining pressure is unloaded completely.

Influences of different unloading rates on deformation parameters

In the stress–strain curve of the uniaxial compression test, the tangent modulus of initial load generally characterizes elastic characteristics of the materials under very low stress. This modulus (expressed as E_0) is determined by inclination of the tangent line at the starting point of the stress–strain curve of the uniaxial compression test, which is used to analyze the effects of loading modes on performance of granite in this study. The confining pressure unloading rate has little influence on the elastic modulus of rock samples at the initial stage of confining pressure unloading, but has obvious influence on rock failure (Chai and Li 2011). The changes of tangent modulus at initial load in the whole unloading test in different stages of the four groups are shown in Fig. 10a–d. It can be found from the four figures that the change trends of tangent moduli at initial load are same and the value increases all the time in the stage of loading confining and axial pressures. When beginning to unload confining

pressure, the value of tangent moduli sharply drops and then attenuates with leaps with the constant decrease of confining pressure. Under conditions of using different unloading modes in different stages, distinct forms of attenuation with leaps can be observed. Figure 10e demonstrates changes of tangent moduli at initial load in the failure process under UCP and conventional TC. It can be observed from Fig. 10e that tangent moduli at initial load of the thermally subjected rock samples change differently in the failure process under conventional TC and UCP. In the UCP test, the value rises to the maximum in the loading stage, followed by a sharp drop when confining pressure begins to be unloaded, and then it attenuates with leaps with unloading of confining pressure. In the conventional TC test, the value firstly rises and then reduces: it gradually decreases as the test proceeds after rising to a certain value. This indicates that such a change trend of stress has greater influences on mechanical performance of the granite during the UCP test compared with the conventional TC test.

In addition to tangent modulus at initial load, there are another two important mechanical parameters for the rock, i.e. elastic modulus and Poisson’s ratio. Elastic modulus in rock mechanics is generally calculated in elastic stage in

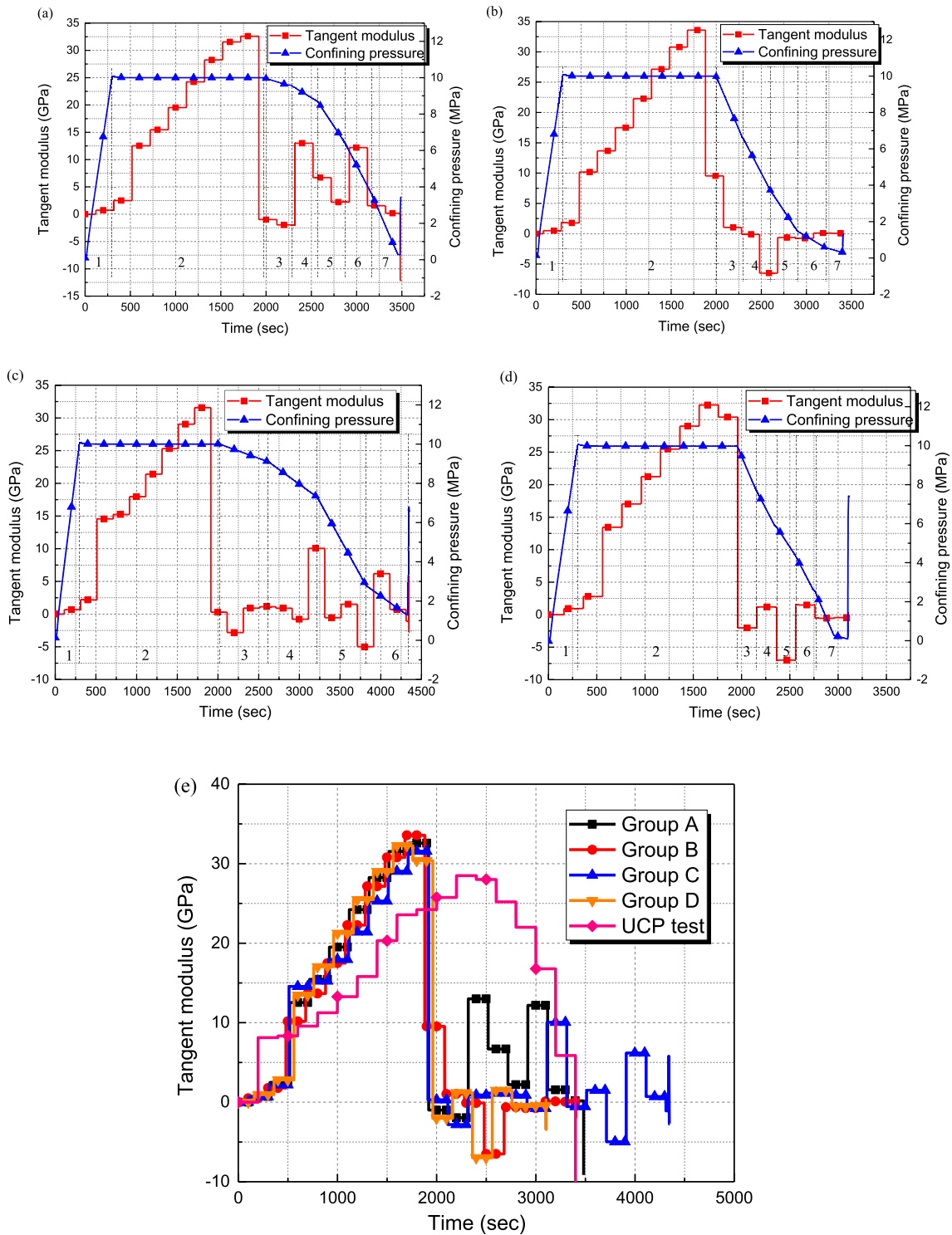


Fig. 10 Change characteristics of tangent moduli during unloading of confining pressure

uniaxial or TC test, while calculation of deformation parameters during unloading of confining pressure should comprehensively considers effects of stress and strain in each direction. In accordance with the generalized Hooke’s law, it is assumed that each stress and deformation point on the

stress–strain curve of the rock during unloading damage and failure still confirms to the general Hooke’s law. Based on this, Huang (2010) solved deformation parameters during deformation and failure in the unloading process, so as to understand weakening laws of deformation parameters

during unloading. The formula for solving deformation parameters through the generalized Hooke’s law is shown as follows:

$$E = \frac{\sigma_1 - 2\mu\sigma_a}{\epsilon_1} \tag{2}$$

$$\mu = \frac{(B\sigma_1 - \sigma_3)}{[\sigma_3(2B - 1) - \sigma_1]} \tag{3}$$

$$B = \frac{\epsilon_3}{\epsilon_1}. \tag{4}$$

Figure 11 demonstrates change characteristics of elastic modulus with confining pressure during unloading of confining pressure. As shown in Fig. 11a, the initial elastic moduli under unloading in the four test groups are different, while change trends thereof are basically same in various groups at UCP rates in different stages, shown as linear decreases of deformation parameter in the initial unloading stage with

the reduction of confining pressure. When unloading to the failure point, deformation parameter dramatically decreases. In order to compare differences in changes of elastic moduli during unloading of confining pressure in the four test groups, the initial elastic moduli of the four curves are rendered same through normalization without changing change trends of each curve, as shown in Fig. 11b. By comparing change curves of elastic moduli under different modes of UCP in different stages in Fig. 11b, elastic modulus changes more obviously and decrease rate of elastic modulus in the initial unloading stage (among the three stages) in the test group C is larger than those in the other three test groups. This indicates that the rock changes largely in parameter of elastic modulus and is most easily damaged under such a UCP mode in different stages.

Change curves of Poisson’s ratio of the granite with confining pressure during unloading of confining pressure are demonstrated in Fig. 12. In the figure, during unloading of confining pressure under the path without changing deviatoric stress, Poisson’s ratio of the rock samples changes gently (basically from 0.4 to 0.45) and decreases in the initial period. However, when the unloading-induced failure is about to occur, it decreases rapidly and exponentially. The reason for such changes of Poisson’s ratio is that when confining pressure is unloaded under constant deviatoric stress, axial deformation changes slowly, while radial deformation continuously varies from positive strain to negative strain. Poisson’s ratio is shown as the effects generated by radial strain in axial direction, so it continuously reduces with the decrease of confining pressure in the test process.

Impacts of different unloading rates on strain-pressure compliance

The change relationship between confining pressure and volumetric strain during unloading of confining pressure in different stages was analyzed in “Effects of different unloading rates on the relationship between confining pressure and strain”. It is obtained that in the four groups of unloading tests in different stages, magnitude of unloading of confining pressure of the granite is the minimum in the test group C and the rock samples in the group are most easily damaged. Furthermore, unloading-induced failure of the granite samples is caused by rapid volume expansion. The change laws of deformation parameters of the thermally subjected granite samples during failure under UCP were discussed in “Influences of different unloading rates on deformation parameters”. This and the following sections mainly discussed the interaction between confining pressure and strain during unloading of the granite and change laws of expansion characteristics of the rock samples in the unloading-induced failure process.

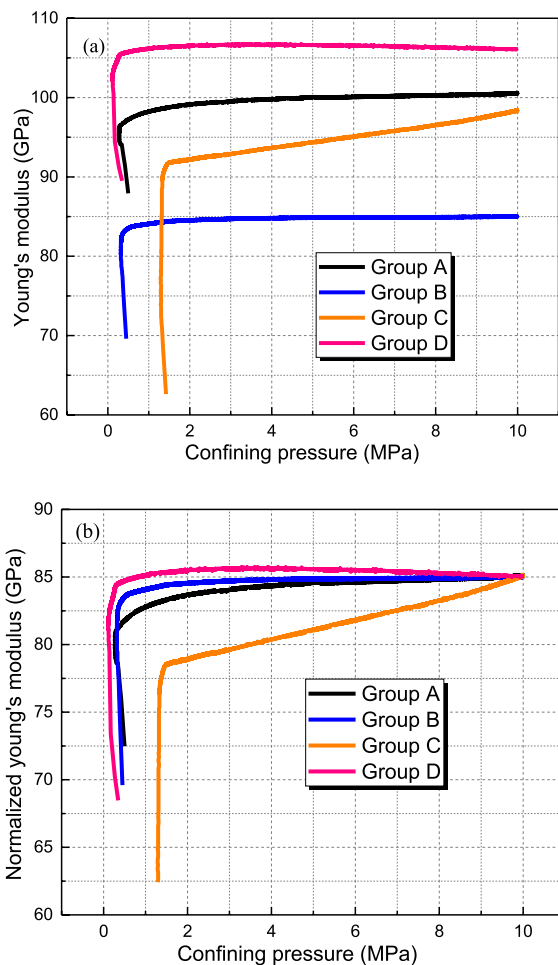


Fig. 11 Change characteristics of elastic moduli during unloading of confining pressure

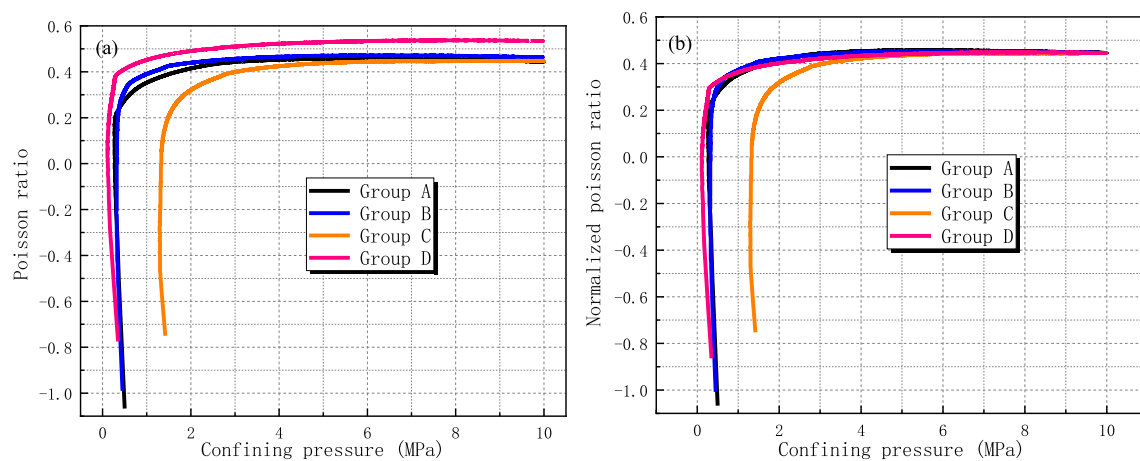


Fig. 12 Change characteristics of Poisson's ratio during unloading of confining pressure

In order to analyze rock deformation during unloading, this study introduced strain-pressure compliance proposed by Qiu (2010) for description. The strain-pressure compliance $\Delta\dot{\epsilon}_i$ refers to the ratio of strain increment caused by UCP to decrease of confining pressure between the starting point of UCP and the point of stress drop, which is expressed as follows:

$$\Delta\dot{\epsilon}_i = \frac{\Delta\epsilon_i}{\Delta\sigma_3}, \quad (5)$$

where $\Delta\epsilon_i$ ($i = 1, 3, v$) separately represent the axial, circumferential and volumetric strain increments. The strain-pressure compliance $\Delta\dot{\epsilon}_i$ is a physical quantity to measure the change speed of each deformation increment under per unit decrease of confining pressure, which better reflects the effects of changes of confining pressure on deformation during unloading and shows the response speed of internal structure of the rock to change process of stress state. The larger the strain-pressure compliance $\Delta\dot{\epsilon}_i$ is, the more sensitive the deformation in a certain direction to decrease of confining pressure.

In accordance with the test results, the axial, radial and volumetric strain-pressure compliances of the granite samples from the starting point of unloading to failure of the rock samples shown in Fig. 13 are calculated by using Formula (5). Yang (2017) concluded that the peak stress increase rate of the rock sample increases with the initial confining pressure. Figure 13a–c demonstrates magnitudes of axial, radial and volumetric strain-pressure compliances corresponding to different unloading stages in the UCP process in the four test groups. Figure 13d shows the magnitude of strain-pressure compliance in the whole process from beginning of unloading to the end of failure of the rock samples. As illustrated in Fig. 13a–c, the three strain-pressure compliances all rise as the unloading proceeds, and they change

stably in the first three stages of unloading while increase rapidly from the fourth stage till the samples are damaged. It can be obviously seen that strain-pressure compliance of the rock samples in the test group C sharply enlarges from the third stage compared with the other three test groups and it is more than ten times that of the rock samples in the other three test groups in the same stage. Moreover, the rock samples in this group are damaged by only undergoing the first four stages. Strain-pressure compliances in the test groups, respectively, B and D group trials and the smallest one is found in the test group A. This indicates that the samples in the test group A are the least easily damaged under the mode of changing UCP rates in different stages and that the UCP test in different stages under change modes of different unloading rates exerts dissimilar influences on rock strength. In practical engineering, deep rocks affected by high temperatures are subjected to different stress perturbations. In addition, different stress perturbations will produce different unloading rates around the rock, which will cause different failures to the rock. As illustrated in Fig. 13d, during UCP of the granite, the UCP rate has obvious effects on axial, radial and volumetric strains of the rock. Compared with radial and volumetric strain-pressure compliances, axial strain-pressure compliance is smallest. This means that different unloading rates exert the smallest influences on axial deformation during the whole UCP test of the rock; on the contrary, radial and volumetric deformation responds more sensitively to changes of confining pressure than axial deformation.

Change laws of expansion characteristics of the granite

Analysis in the above sections reveals that the granite samples obviously expand in the UCP test. Li (1993) explained such a phenomenon as the result of the superposition of a lateral tensile stress on the original stress state under UCP

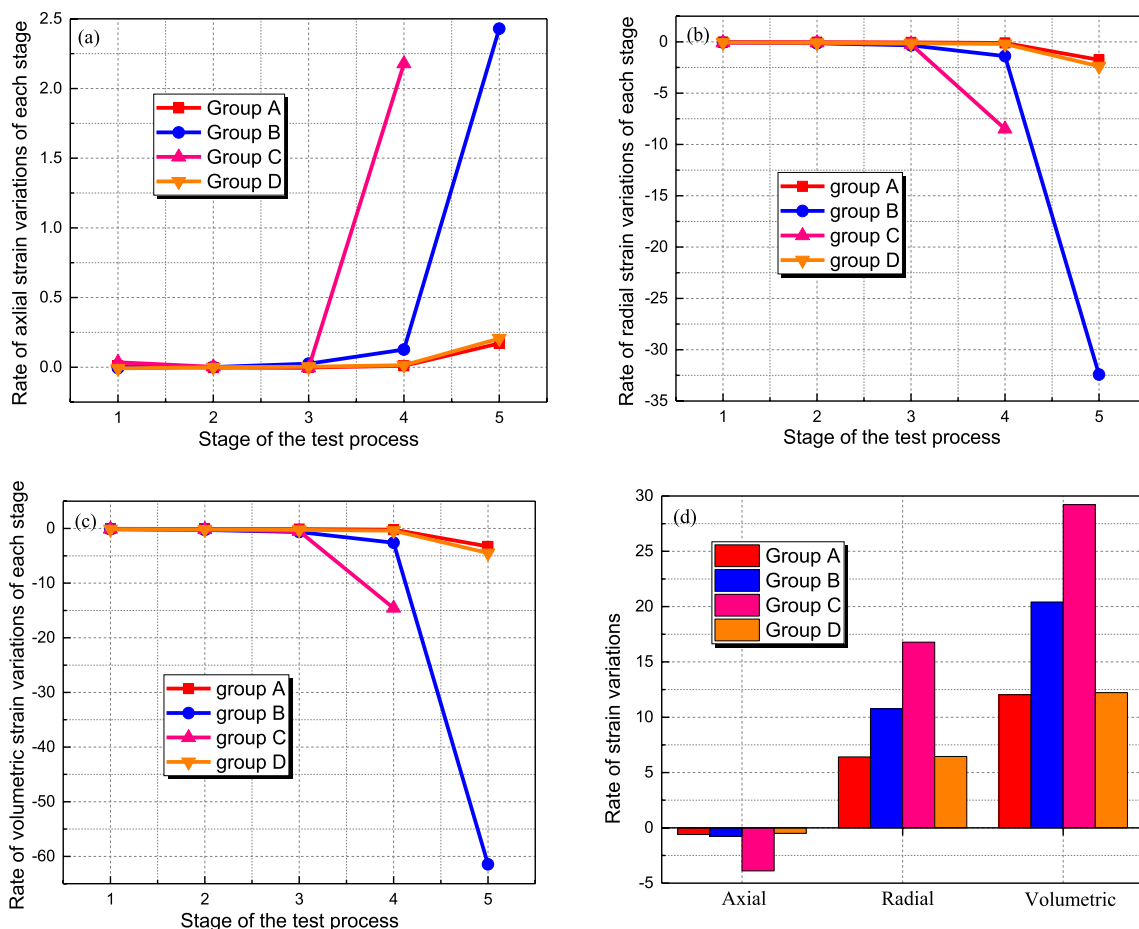


Fig. 13 Strain-pressure compliance of the rock samples in the UCP stage

of the rock. Vermeer (1984) suggested to use dilatancy angle ψ in the plastic theory to characterize inelastic volume change by utilizing Formula (6).

$$\psi = \arcsin\left(\frac{\dot{\epsilon}_V^P}{-2\dot{\epsilon}_1^P + \dot{\epsilon}_V^P}\right), \tag{6}$$

where $\dot{\epsilon}_1^P$ and $\dot{\epsilon}_V^P$ represent the increments of axial and volumetric plastic strains during UCP of the rock samples, respectively.

Detournay (1986) proposed to take dilatancy angle ψ as the function of plastic parameter and confining pressure and the plastic parameter generally values plastic shear strain, namely,

$$\gamma^P = \epsilon_1^P - \epsilon_3^P. \tag{7}$$

Therefore, this study also adopted the same method to analyze change laws of dilatancy angle ψ with plastic shear strain γ^P .

Elastic constants refer to Young’s modulus E and Poisson’s ratio ν , which are generally obtained in the elastic deformation stage before unloading stage on the stress–strain curve. According to characteristics of curves in Fig. 8, elastic constants are calculated in the range of 70–85% of the maximum deviatoric stress on the stress–strain curve. Assuming that elastic constants are unchanged all the time during unloading in the UCP test of the granite, elastic axial strain ϵ_1^e and elastic volumetric strain ϵ_v^e can be calculated according to the theory of elastic mechanics. Furthermore, plastic shear strain is calculated based on the following formula.

$$\epsilon_1^e = \frac{\sigma_1 - 2\nu\sigma_3}{E} \tag{8}$$

$$\epsilon_v^e = \frac{(1 - 2\nu)\sigma_1 - 2(1 - \nu)\sigma_3}{E} \tag{9}$$

$$\varepsilon_1^p = \varepsilon_1 - \varepsilon_1^e, \varepsilon_v^p = \varepsilon_v - \varepsilon_v^e. \quad (10)$$

The change curves of the dilatancy angle with plastic shear strain increment during unloading in the four UCP tests calculated according to the above Formulas (6–10) are shown in Fig. 14. The following conclusions are made according to Fig. 14.

1. At the end of elastic deformation stage and before unloading, initial dilatancy angles in each group are basically same. According to the test steps in “Test procedures”, the loading modes for confining and axial pressures and magnitudes of confining pressure are same in the four test groups. Therefore, after the rock samples experience loading stage, changes of dilatancy angle are basically same.
2. The evolution process of dilatancy angle is basically same regardless of the unloading mode of the confining pressure in different stages. The dilatancy angle increases rapidly to a certain value in the initial stage of unloading, which is about three times that of the original value. Under different modes of UCP in different stages, plastic shear strains with the dilatancy angle reaching this value are approximately same, which undergoes the first three stages. From the fourth stage, dilatancy angles of the rock samples in different test groups show distinct change trends, while the general trend is that the dilatancy angle rises to the maximum and rapidly drops with constant decrease of confining pressure. In this case, the rock samples are damaged. Such a change trend is inconsistent with the conclusion obtained by Qiu (2010), that is, the dilatancy angle keeps unchanged after reaching a certain value till the rock samples are

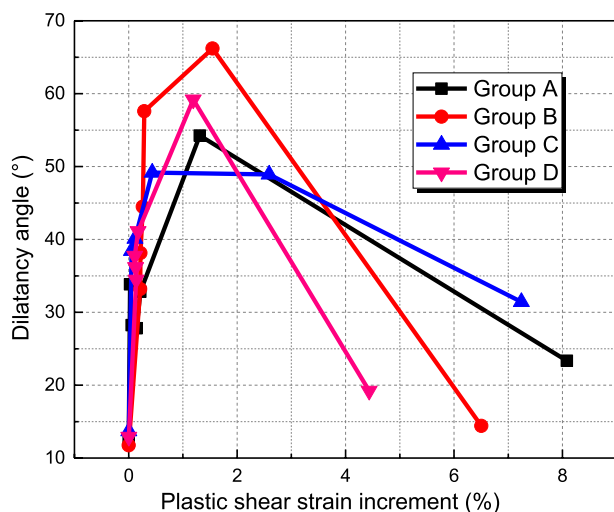


Fig. 14 Change laws of dilatancy angle of the granite during unloading in the UCP test

damaged. The main reason is probably that stress path during unloading of confining pressure is not same with that of Qiu. This study is based on the constant deviatoric stress ($\sigma_1 - \sigma_3$), while the test of Qiu is based on unchanged σ_1 . As to different evolution laws of dilatancy angles under different stress paths, it remains to be further studied.

3. By combining with Table 2, under UCP at a low rate (test groups A and C), peak dilatancy angles are lower than that under UCP at a high rate (test groups B and D), which is consistent with the conclusion made by Qiu (2010). In other words, under UCP at a low rate, the dilatancy angle of the rock samples firstly reaches the peak and then decreases. When the rock samples are damaged, the dilatancy angle rapidly drops.

Conclusions

By utilizing the RTX-3000 high-temperature and high-pressure triaxial rock testing machine, the conventional TC test and triaxial UCP test were conducted under constant deviatoric stress on the granite samples after being subjected at 800 °C and naturally cooled. On this basis, the mechanical properties of the granite during failure under UCP were studied and the main conclusions are made as follows:

1. SEM analysis results of the granite samples thermally subjected at 800 °C show that many intergranular cracks appear in the rock samples and the microstructures are damaged to some extent due to high-temperature thermal stress. Compared with the conventional TC test, there is no obvious peak point on the curve, while an obvious yield platform appears and the curve is nearly flat during the UCP test on the rock samples. With the decrease of confining pressure, the original cracks in the samples propagate and coalesce, or new cracks initiate. Moreover, the rock expands and deformation dramatically increases after confining pressure is reduced to a certain degree. Therefore, the points of obvious stress drop can be observed and the rock shows obvious characteristics of brittle failure.
2. In the initial unloading stage of confining pressure on the rock samples, volumetric strain rises slightly. With the gradual decrease of confining pressure, the relationship between volumetric strain and confining pressure is not linear any more. As confining pressure is reduced to a certain degree, volumetric strain rapidly increases till the rock samples are damaged, and the rock samples in the test group C show the largest expansion and are most likely to be damaged. The dilatancy angle is used to quantitatively describe such a volume expansion phenomenon, shown as follows: the dilatancy angle rapidly

rises with the reduction of confining pressure and then immediately rapidly drops after reaching a certain value during unloading of confining pressure under constant deviatoric stress of the rock samples. The peak dilatancy angle in the test group C is the smallest in the four test groups, that is, it firstly reaches the peak.

3. The strain-pressure compliance of the rock samples in the UCP test in different stages changes basically in a same manner. The strain-pressure compliances of the samples in the first three stages in each test group are almost no change and rapidly increase from the fourth stage till the rock samples are damaged. This indicates that internal structure of the rock begins to respond to the change of confining pressure from the fourth stage during the UCP test of the granite samples, implying that internal structure of the rock samples has not been largely changed in the initial unloading stage. In comparison with the changes of axial strain-pressure compliance, radial and volumetric strain-pressure compliances are much larger, which reflects that radial strain is more sensitive to the changes of confining pressure.
4. Different from the phenomenon that tangent modulus of the rock samples firstly increases and then decreases in the conventional TC test, the tangent modulus in the UCP test in different stages rapidly reduces at the beginning of unloading and then attenuates with leaps as confining pressure is decreased. Elastic modulus and Poisson's ratio of the rock samples show a same change trend during unloading of confining pressure and change slightly in the initial unloading stage. As confining pressure is reduced further, they rapidly reduce till the rock samples are damaged. The elastic modulus and Poisson's ratio in the test group C firstly drop, the confining pressure of rock samples in group C has been reduced by 87%, suggesting that the rock samples in this test group are most likely to be damaged under UCP (unloading rate firstly rises and then reduces) in different stages.

Funding This work was funded by the National Natural Science Foundation of China (51974043), Key Projects of Teaching Reform in Hunan Province in 2022 (HNJG-2022-0031), and 2022 Young Science and Technology Talent Program & Hunan Young Talent Program (2022RC1173), which are gratefully acknowledged. The authors also thank the editor and anonymous reviewers for their valuable advice.

Data availability Some or all of the data, models, or code generated or used during the study are available from the corresponding author by request.

Declarations

Conflict of interest The authors declare that they have no conflicts of interest in this work. We declare that we do not have any commercial

or associated interests that represent conflicts of interest in connection with the work submitted.

References

- Aversa S, Evangelista A (1998) The mechanical behaviour of a pyroclastic rock: yield strength and “destruction” effects. *Rock Mech Rock Eng* 31(1):25–42
- Brotons V, Tomás R, Ivorra S et al (2013) Temperature influence on the physical and mechanical properties of a porous rock: San Julian's calcarenite. *Eng Geol* 167:117–127
- Cevik A, Sezer EA, Cabalar AF, Gokceoglu C (2011) Modelling of the uniaxial compressive strength of some clay-bearing rocks using neural network. *Appl Soft Comput* 11(2):2587–2594
- Chai WG, Li WL (2011) Research on influences of unloading rate on rock damage and failure under confining pressure unloading. *Appl Mech Mater* 71–78:1565–1571
- Chaki S, Takarli M, Agbodjan WP (2008) Influence of thermal damage on physical properties of a granite rock: porosity, permeability and ultrasonic wave evolutions. *Constr Build Mater* 22(7):1456–1461
- Deng HF, Wang Z, Li JL, Jiang Q, Zhang HB (2017) Effect of unloading rate and pore water pressure on mechanical properties of sandstone. *Chin J Geotech Eng* 39(11):1976–1983
- Detournay E (1986) Elastoplastic model of a deep tunnel for a rock with variable dilatancy. *Rock Mech Rock Eng* 19(2):99–108
- Dobson DP, Meredith PG, Boon SA (2002) Simulation of subduction zone seismicity by dehydration of serpentine. *Science* 298(5597):1407–1410
- Dong LJ, Chen YC, Sun DY, Zhang YH (2021) Implications for rock instability precursors and principal stress direction from rock acoustic experiments. *Int J Min Sci Technol* 31(05):789–798
- Dou L, Yang K, Chi X (2021) Fracture behavior and acoustic emission characteristics of sandstone samples with inclined precracks. *Int J Coal Sci Technol* 8(1):77–87
- Franklin JA, Vogler UW, Szlavins J (1979) Suggested methods for determining water content, porosity, density, absorption and related properties and swelling and slake-durability index properties: part 1: suggested methods for determining water content, porosity, density, absorption and related properties. *Int J Rock Mech Min Sci* 16:143–151
- Hashemi SS, Melkounian N, Taheri A (2015) A borehole stability study by newly designed laboratory tests on thick-walled hollow cylinders. *J Rock Mech Geotech Eng* 7(5):519–531
- HouPert R (1979) *Proe. 4th Int. Congr. Rock Mech. Montreux* 3:104–114
- Huang RQ, Huang D (2010) Experimental research on affection laws of unloading rates on mechanical properties of Jinping marble under high geostress. *Chin J Rock Mech Eng* 29(1):21–33
- Kayabasi A, Gokceoglu C, Ercanoglu M (2003) Estimating the deformation modulus of rock masses: a comparative study. *Int J Rock Mech Min Sci* 40(2003):55–63
- Kim BH, Walton G, Larson MK, Berry S (2021) Investigation of the anisotropic confinement-dependent brittleness of a Utah coal. *Int J Coal Sci Technol* 8(2):274–290
- Lau JSO, Chandler NA (2004) Innovative laboratory testing. *Int J Rock Mech Min Sci* 41(8):1427–1445
- Lau JS O, Gorski B, Jackson R (1995) The effects of temperature and water-saturational on mechanical Properties of Lacdu Bonnet pink granite. 8th Int.Con.On Rock Mech, Tokyo, JaPan.
- Liu S, Xu J (2014) Mechanical properties of Qinling biotite granite after high temperature treatment. *Int J Rock Mech Min Sci* 71:188–193
- Liu B, Zhao Y, Zhang C, Zhou JL, Li Y, Sun Z (2021a) Characteristic strength and acoustic emission properties of weakly cemented

- sandstone at different depths under uniaxial compression. *Int J Coal Sci Technol* 8(6):1351–1370. <https://doi.org/10.1007/s40789-021-00462-0>
- Liu XS, Song SL, Tan YL, Fan DY, Ning JG, Li XB, Yin YC (2021b) Similar simulation study on the deformation and failure of surrounding rock of a large section chamber group under dynamic loading. *Int J Min Sci Technol* 31:495–505
- Meng L, Li T, Liao A (2018) Anisotropic mechanical properties of sandstone under unloading confining pressure at high temperatures. *Arab J Sci Eng* 1:1–12
- Nasseri MHB, Tatone BSA, Grasselli G, Young RP (2009) Fracture toughness and fracture roughness interrelationship in thermally treated Westerly Granite. *Pure Appl Geophys* 166:801–822
- Peng K, Zhou J, Q, (2019) Effects of stress lower limit during cyclic loading and unloading on deformation characteristics of sandstones. *Constr Build Mater* 217:202–215
- Popov Y, Beardsmore G, Clauser C, Roy S (2016) ISRM suggested methods for determining thermal properties of rocks from laboratory tests at atmospheric pressure. *Rock Mech Rock Eng* 49:1–29
- Qiu SL, Feng XT, Zhang CZ, Zhou H, Sun F (2010) Experimental research on mechanical properties of deep-buried marble under different unloading rates of confining pressures. *Chin J Rock Mech Eng* 29(9):1807–1817
- Ranjan K, Prabhat K, Narayan AJ (2021) Das. Evaluation of load transfer mechanism under axial loads in a novel coupler of dual height rock bolts. *Int J Min Sci Technol* 31:225–232
- Tianbin Li, Lansheng W (1993) An experimental study on deformation and failure features of a basalt under unloading condition. *Chin J Rock Mech Eng* 12(4):321–327
- Tsang C-F, Bernier F, Davies C (2005) Geohydromechanical processes in the excavation damaged zone in crystalline rock, rock salt, and indurate and plastic clays: In the context of radioactive waste disposal. *Int J Rock Mech Min Sci* 42(1):109–125
- Vázquez P, Shushakova V, Gómez-Heras M (2015) Influence of mineralogy on granite decay induced by temperature increase: experimental observations and stress simulation. *Eng Geol* 189:58–67
- Vermeer PA, de Borst R (1984) Non-associated plasticity for soils, concrete and rock. Delft University of Technology, Heron
- Witherspoon PA (2006) Geological problems in radioactive waste isolation: The 4th World Wide Review (LBNL- 59808). Lawrence Berkeley National Laboratory, California, pp 55–64
- Witherspoon PA (2011) Geological problems in radioactive waste isolation: The 3rd World Wide Review (LBNL- 38915). Lawrence Berkeley National Laboratory, California, pp 77–84
- Wong TE (1982) Effects of temperature and pressure on failure and post-failure behavior of westerly granite. *Mech Mater* 1(3):17
- Wu G, Zhang L (2004) Studying unloading failure characteristics of a rock mass using disturbed state concept. *Int J Rock Mech Min Sci* 41(S1):181–187
- Xie HQ, He CH (2004) Study of the unloading characteristics of a rock mass using the triaxial test and damage mechanics. *Int J Rock Mech Min Sci* 41:13–18
- Xu XC, Liu QS (2000) A preliminary study on basic mechanical properties for granite at high temperature. *Chinese Journal of Geotechnical Engineering* 22(3):276–278
- Yang Y, Xie H, Xiao M (2017) Deformation failure and energy characteristics of transverse-isotropic rock under unloading of high confining pressure. *Chin J Rock Mech Eng* 36(8):1999–2006
- Yu QL, Ranjith PG, Liu HY, Yang TH, Tang SB, Tang CA, Yang SQ (2015) A mesostructure-based damage model for thermal cracking analysis and application in granite at elevated temperatures. *Rock Mech Rock Eng* 48(6):2263–2282
- Yu C, Ji S, Li Q (2016) Effects of porosity on seismic velocities, elastic moduli and Poisson's ratios of solid materials and rocks. *J Rock Mech Geotech Eng* 8(1):35–49
- Zou QL, Liu H, Jiang ZB, Wu X (2021) Gas flow laws in coal subjected to hydraulic slotting and a prediction model for its permeability-enhancing effect. *Energy Sour Part A Recover Utilization Environ Eff*. <https://doi.org/10.1080/15567036.2021.1936692>
- Zou QL, Zhang TC, Cheng ZH, Jiang ZB, Tian SH (2022a) A method for selection rationality evaluation of the first-mining seam in multi-seam mining. *Geomech Geophys Geo-Energy Geo-Resour* 8:17
- Zou QL, Zhang TC, Ma TF, Tian SX, Jia XQ, Jiang ZB (2022b) Effect of water-based SiO₂ nanofluid on surface wettability of raw coal. *Energy* 254:124228
- Zou QL, Zhou XL, Wang RZ, Ning YH, Chen ZH, Kong FJ, Liu Y (2022c) Load-carrying and energy-absorbing performance of honeycombs with different cross sections under cyclic loading. *Mater Today Commun* 33:104582

Publisher's Note Springer Nature remains neutral with regard to jurisdictional claims in published maps and institutional affiliations.

Springer Nature or its licensor (e.g. a society or other partner) holds exclusive rights to this article under a publishing agreement with the author(s) or other rightsholder(s); author self-archiving of the accepted manuscript version of this article is solely governed by the terms of such publishing agreement and applicable law.